Synthetic Metals xxx (2015) xxx–xxx

Contents lists available at ScienceDirect

Synthetic Metals

journal homepage: www.elsevier.com/locate/synmet

Graphene controlled organic photodetectors

Q1 A. Mekki[a], A. Dere[b], Kwadwo Mensah-Darkwa[c], Ahmed Al-Ghamdi[d], R.K. Gupta[e,**], K. Harrabi[a], W.A. Farooq[f], Farid El-Tantawy[g,h], F. Yakuphanoglu[a,d,*]

[a] Department of Physics, King Fahd University of Petroleum & Minerals Dhahran, 31261, Saudi Arabia
[b] Department of Physics, Faculty of Science, Fırat University, Elazig, Turkey
[c] Department of Materials Engineering, College of Engineering, Kwame Nkrumah University of Science and Technology, Kumasi, Ghana
[d] Department of Physics, Faculty of Science, King Abdulaziz University, Jeddah, Saudi Arabia
[e] Department of Chemistry, Pittsburg State University, Pittsburg, KS 66762, USA
[f] Department of Physics and Astronomy, College of Science, King Saud University, Riyadh, Saudi Arabia
[g] Nanoscience and Nanotechnology Laboratory, Firat University, Elazığ, Turkey
[h] Department of Physics, Faculty of Science, Suez Canal University, Ismailia, Egypt

ARTICLE INFO

Article history:
Received 12 February 2016
Received in revised form 6 March 2016
Accepted 11 March 2016
Available online xxx

Keywords:
Solar energy materials
Photodiode
Graphene oxide
Methylene blue

ABSTRACT

Drop casting deposition technique was used to fabricate graphene oxide doped methylene blue (GO doped MB) photodiode, Al/p-Si/GO doped MB/Au. The effects of illumination on the current–voltage (I–V) characteristics of the Al/p-Si/GO doped MB/Au Schottky diode for optical sensing applications were explored. The reverse current of the diode in the reverse bias increases with the increasing illumination intensities. The obtained trends for both ideality factor and barrier height are in agreement, suggesting that they are both affected by GO doping. The photosensitivity of the photodiodes was investigated. The highest photosensitivity was observed for the diode having 0.03 GO:MB ratio with I_{photo}/I_{dark} ratio of 8.67×10^3 at 100 mW/cm^2 under 10 V. The rectification ratio was of the order of 10^4. In addition, the capacitance–voltage (C–V) and conductance–voltage (G–V) measurements of the diode were studied in the frequency range of 10 kHz–1 MHz. The measured values of the capacitance decrease with the increasing frequency. The decrease in capacitance was explained on the basis of interface states. The photoelectrical properties of Al/p-Si/GO doped MB/Au devices indicate that the prepared diodes can be used both as a photodiode and a photocapacitor in optoelectronic device applications.

1. Introduction

The graphite family is well researched material because of its inherent electrical, chemical and mechanical properties, along with its several practical applications [1]. Lots of attention has been given to the exploration of the properties of graphite such as graphene, graphene oxide (GO) and reduced graphene oxide (RGO), for several applications [2–4]. Graphene was discovered by mechanical exfoliation method [5], is a one-atom thick layer of graphite. Many researchers have explored the new world of graphene due to its unique and remarkable electronic properties [6–8], such as high carrier mobility, micron scale mean free path
Q4 and high saturation velocity [9].

Numerous reports have pointed to extensive applications and proposed applications of graphene [2,10–13]. Other reported literature have shown the use of graphene in the development of solar cells and diodes [14,15]. Li et al. [14] used highly conductive semitransparent graphene sheets combined with an n-type silicon wafer to fabricate solar cells with power conversion efficiencies up to 1.5% at AM 1.5 and an illumination intensity of 100 mW cm^{-2}. Lv et al. [16] have used soluble graphene oxide to fabricate graphene films to measure their time-resolved photoconductivity, they observed higher photoconductivity with higher photon energy at same incident light intensity. Xia et al. [10] also used graphene to fabricate photodetectors, and suggested that the generation and transport of photo-carriers in graphene differ fundamentally from those in photodetectors made from conventional semiconductors because of the unique photonic and electronic properties of the graphene. They also demonstrated that the photo response of ultrafast transistor-based photodetectors made from single- and few-layer grapheme does not degrade for optical intensity modulations up to 40 GHz.

Q2 * Corresponding author at: King Fahd University of Petroleum & Minerals Dhahran, Department of Physics, Elazig 31261, Turkey.
Q3 ** Corresponding author.
E-mail addresses: ramguptamsu@gmail.com (R.K. Gupta), fyhanoglu@firat.edu.tr (F. Yakuphanoglu).

http://dx.doi.org/10.1016/j.synthmet.2016.03.015
0379-6779/© 2016 Published by Elsevier B.V.

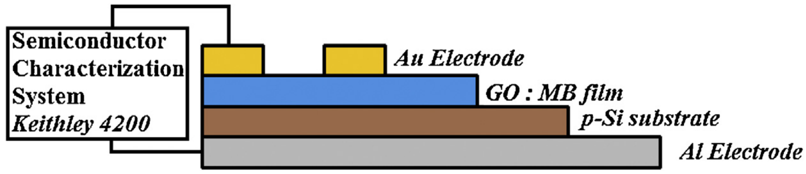

Fig. 1. Schematic diagram of the fabricated device.

Graphene oxide (GO) has emerged as a promising nanomaterial with tremendous potential for photonic applications because of its impressive optical properties [10]. Extensive reports have elaborated on the unique properties of GO such as controllable band gap and high transmittance compared to other graphene-derivatives [17,18]. It must be noted that these properties are essential in the application of optoelectronics. Al-Hartomy et al. [19] have studied the effect of graphene oxide on the diode characteristics of PEDOT-PSS/*p*-Si. It was observed that the diode with 0.1% of GO in the PEDOT:PSS–GO composition had highest photo response property. Also, the *I*–*V* characteristics of the fabricated diodes show strong dependence on composition of GO.

On the other hand, methylene blue (MB) is a blue cationic dye that belongs to the phenothiazine organic family. The absorption of

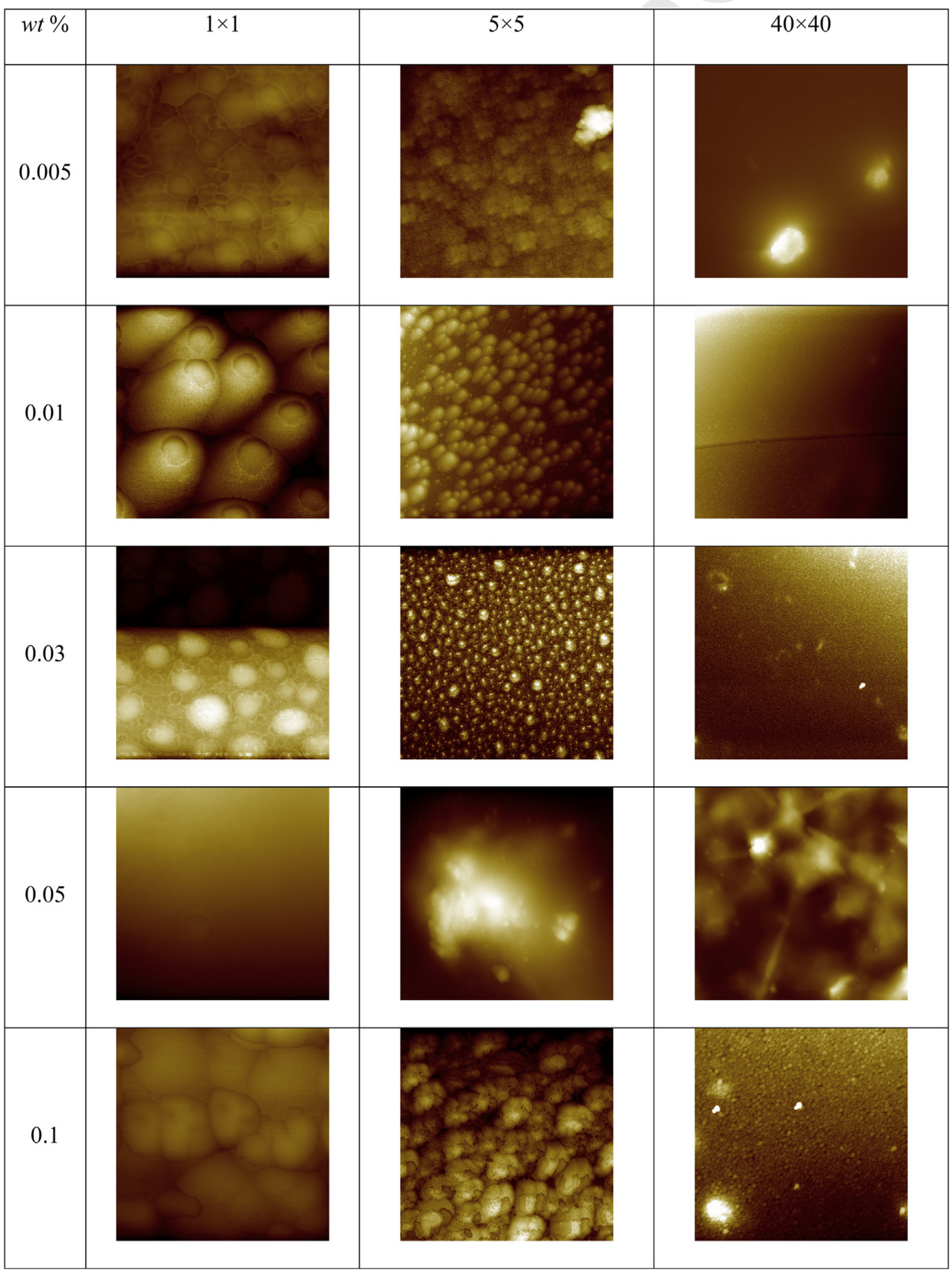

Fig. 2. AFM Images of GO doped MB samples.

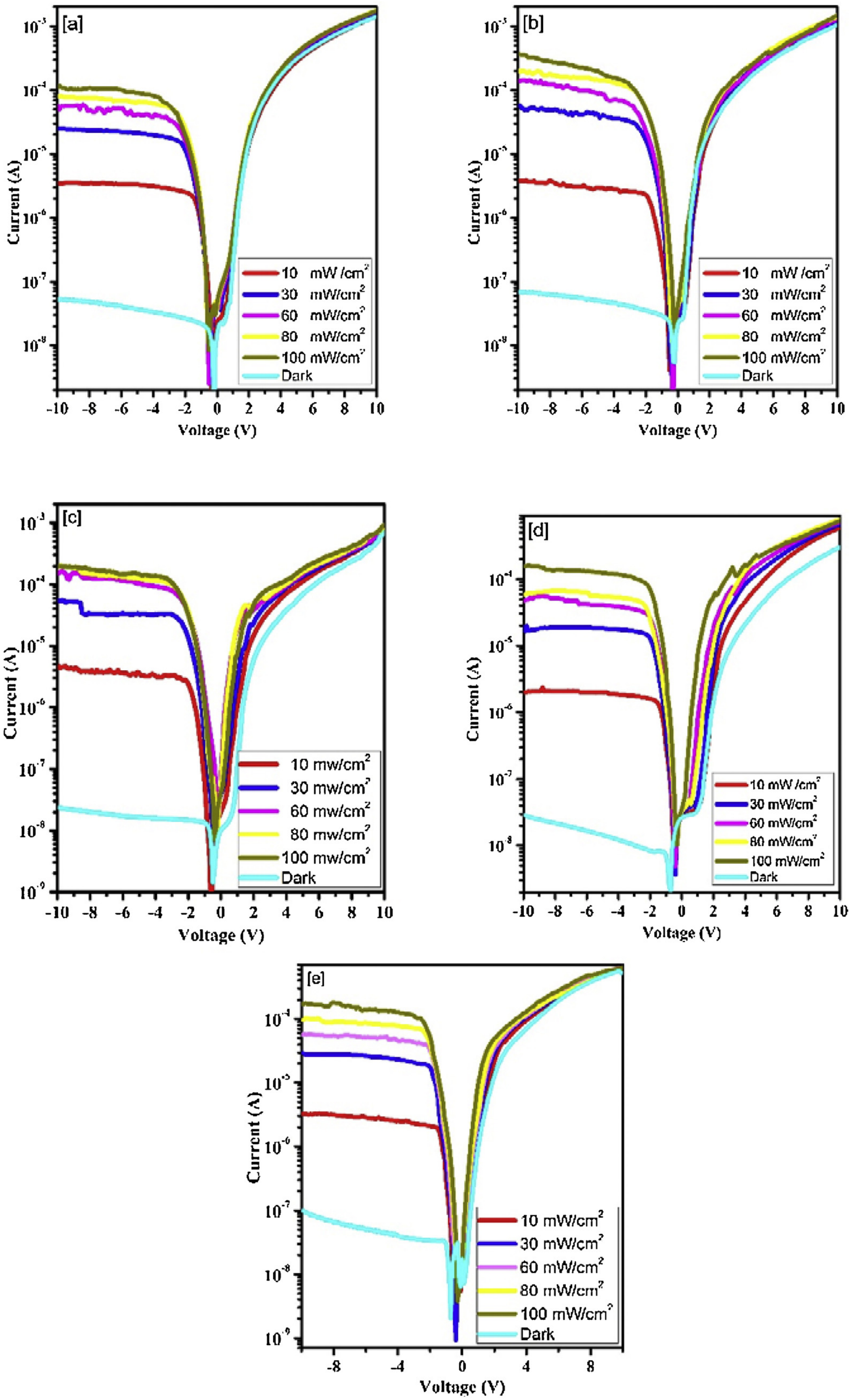

Fig. 3. *I–V* characterization of the fabricated diodes (a) 0.005 (b) 0.01 (c) 0.03 (d) 0.05 (e) 0.1 GO: MB ratio.

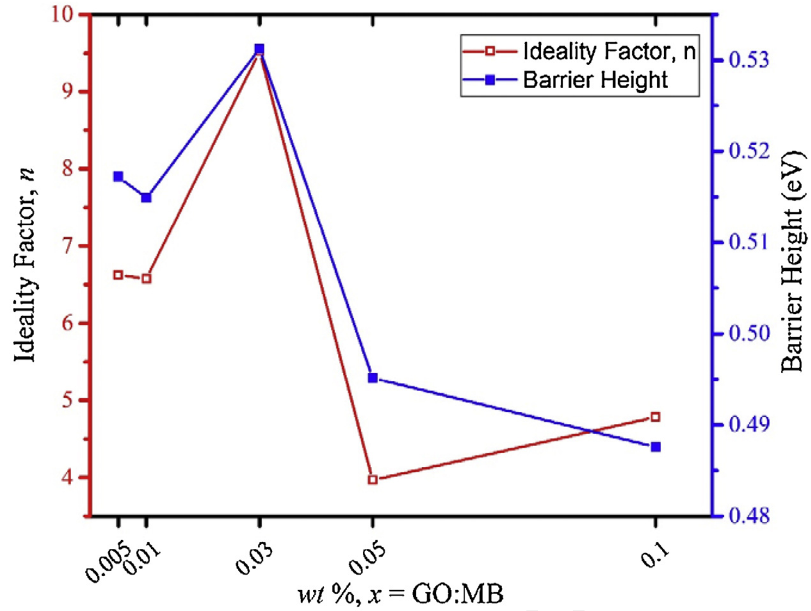

Fig. 4. Plots of GO: MB ratio vs. n and φ_B for the diodes.

Table 1
Photovoltaic parameters of the diodes.

Samples Devices (*wt* %, *x* = GO:MB)	V_{oc} (V)	I_{sc} (A)	I_{photo}/I_{dark} $-10\,V$	*RR*
0.005	−0.23	1.14×10^{-4}	2095	2.60×10^4
0.01	−0.30	3.69×10^{-4}	5182	1.49×10^4
0.03	−0.53	1.93×10^{-4}	8672	3.15×10^4
0.05	−0.68	1.57×10^{-4}	5494	1.04×10^4
0.10	−0.72	1.74×10^{-4}	1744	5.32×10^3

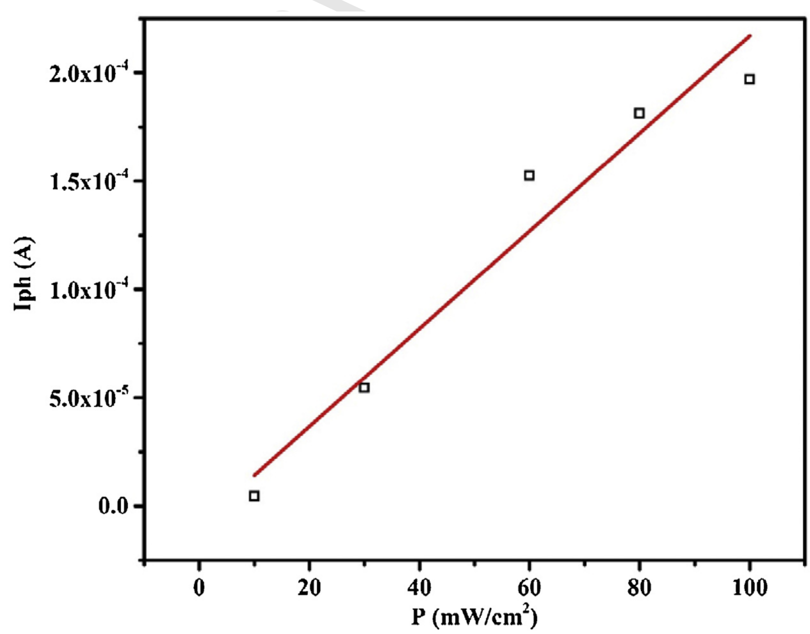

Fig. 5. Plot of I_{ph} vs. P for the diode having 0.03 GO: MB ratio at −10 V.

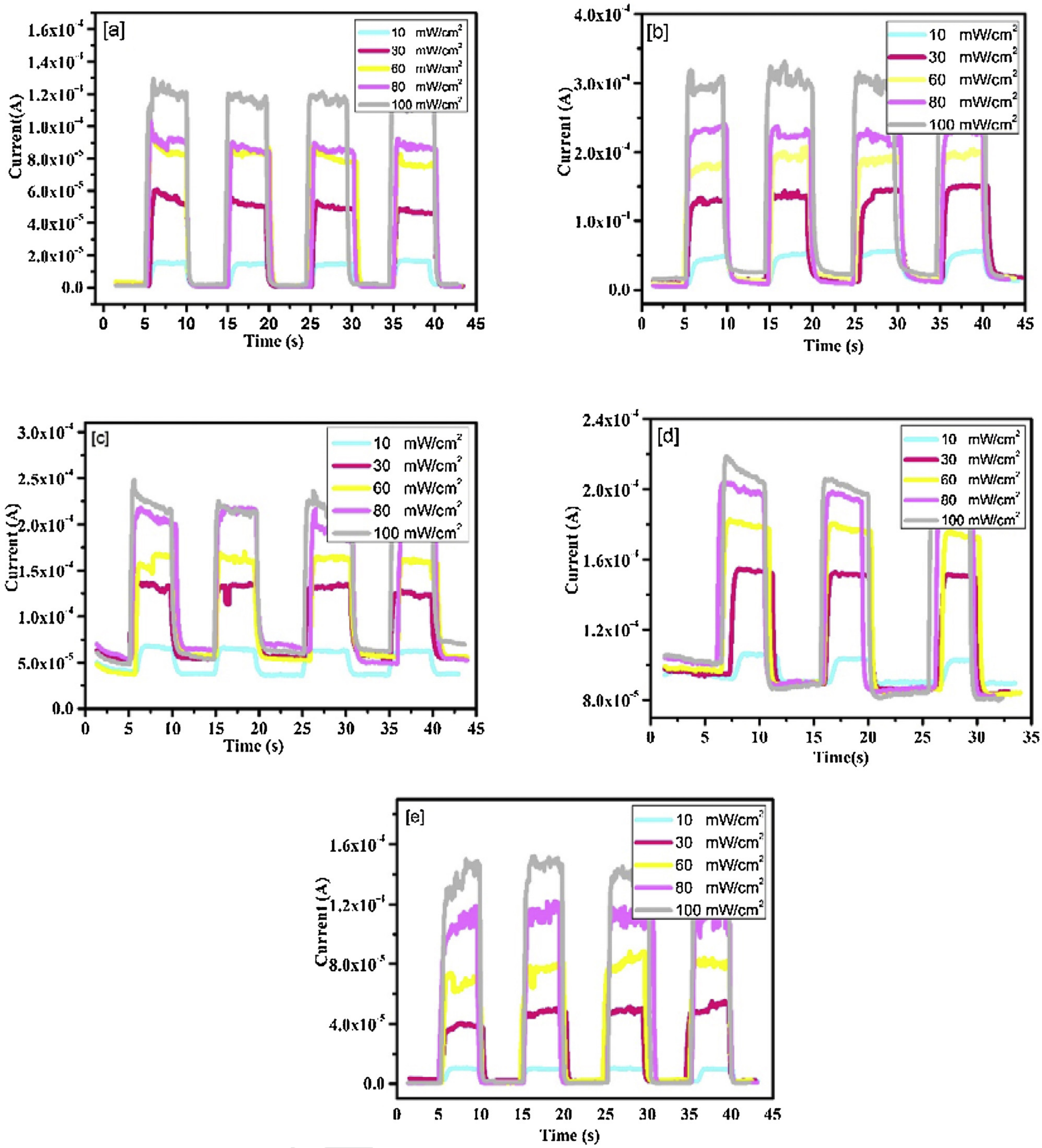

Fig. 6. Transient photocurrent measurements of the photodiode as a function of illumination intensities (a) 0.005 (b) 0.01 (c) 0.03 (d) 0.05 (e) 0.1 GO:MB ratio.

light depends on a number of factors, such as protonation, adsorption to other materials, and metachromasy. It has maximum absorption of light around 670 nm [20]. Zanjanchi and Sohrabnezhad [20] have used MB as an optical humidity sensor, the sensor demonstrated relatively fast response and recovery times about 2 min in the direction of adsorption and about 4 min in the direction of desorption of water. This was explained on the basis of the protonation or deprotonation of the dye molecules.

The motivation of this work is to explore the photovoltaic properties GO doped MB. Herein, we report the on GO doped MB photodiode (Al/p-Si/Go doped MB/Au diode) using drop casting method. The potential of fabricating photovoltaic device having low cost and facile technologies is an extremely important consideration for applications in solar energy converters. The effects of the doping on the optical properties of the devices were studied. The functional properties of photodiodes were investigated to understand the photoconduction properties.

2. Experimental details

GO was prepared from natural graphite using Hummers method reported in [18,21,22]. The methylene blue (MB) was

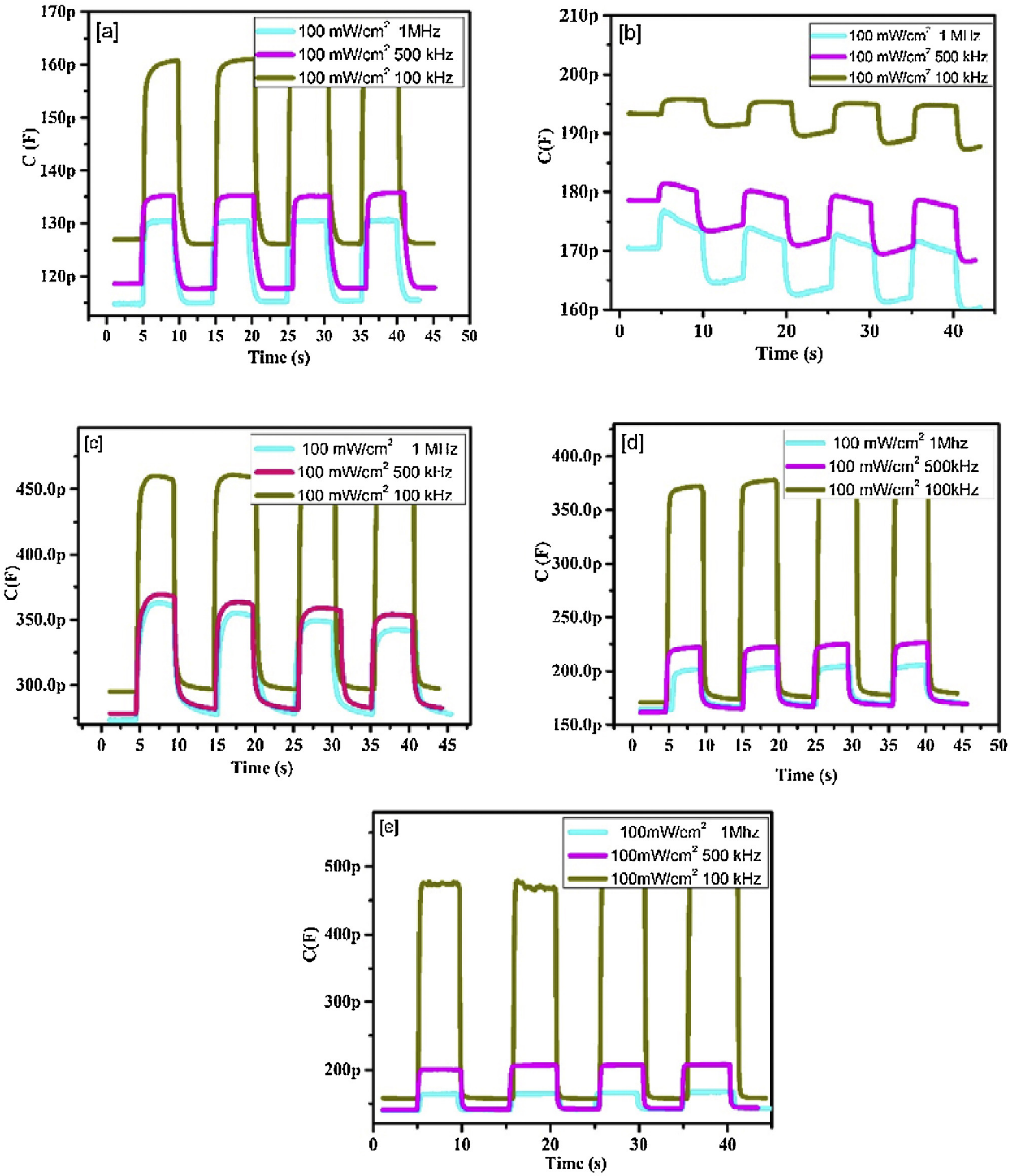

Fig. 7. *C–t* characterization of the fabricated diodes (a) 0.005 (b) 0.01 (c) 0.03 (d) 0.05 (e) 0.1 GO:MB ratio.

dissolved in H_2O and GO was ultrasonically dispersed in H_2O for 2 h. GO doped MB composites were prepared for various weight ratios of (x = GO: MB) (x = 0.005, 0.01, 0.03, 0.05 and 0.10). In order to prepare the diodes, the silicon substrates etched by HF were rinsed in deionized H_2O using an ultrasonic bath for 10–15 min and then, methanol and acetone baths were used to clean the substrates. Ohmic contact having 100 nm was prepared by evaporating Al on o-type silicon at about 10^{-5} Torr and then, the contacts were thermally threated at 570 °C for 5 min in nitrogen atmosphere. GO doped MB solutions of the composites were coated onto surface of p-Si substrate using drop casting method and dried at 50 °C to obtain the solid films. Gold (Au) electrode top contacts were prepared by sputtering system. The diode contact area was found to be 3.14×10^{-2} cm^2. The surface properties of the

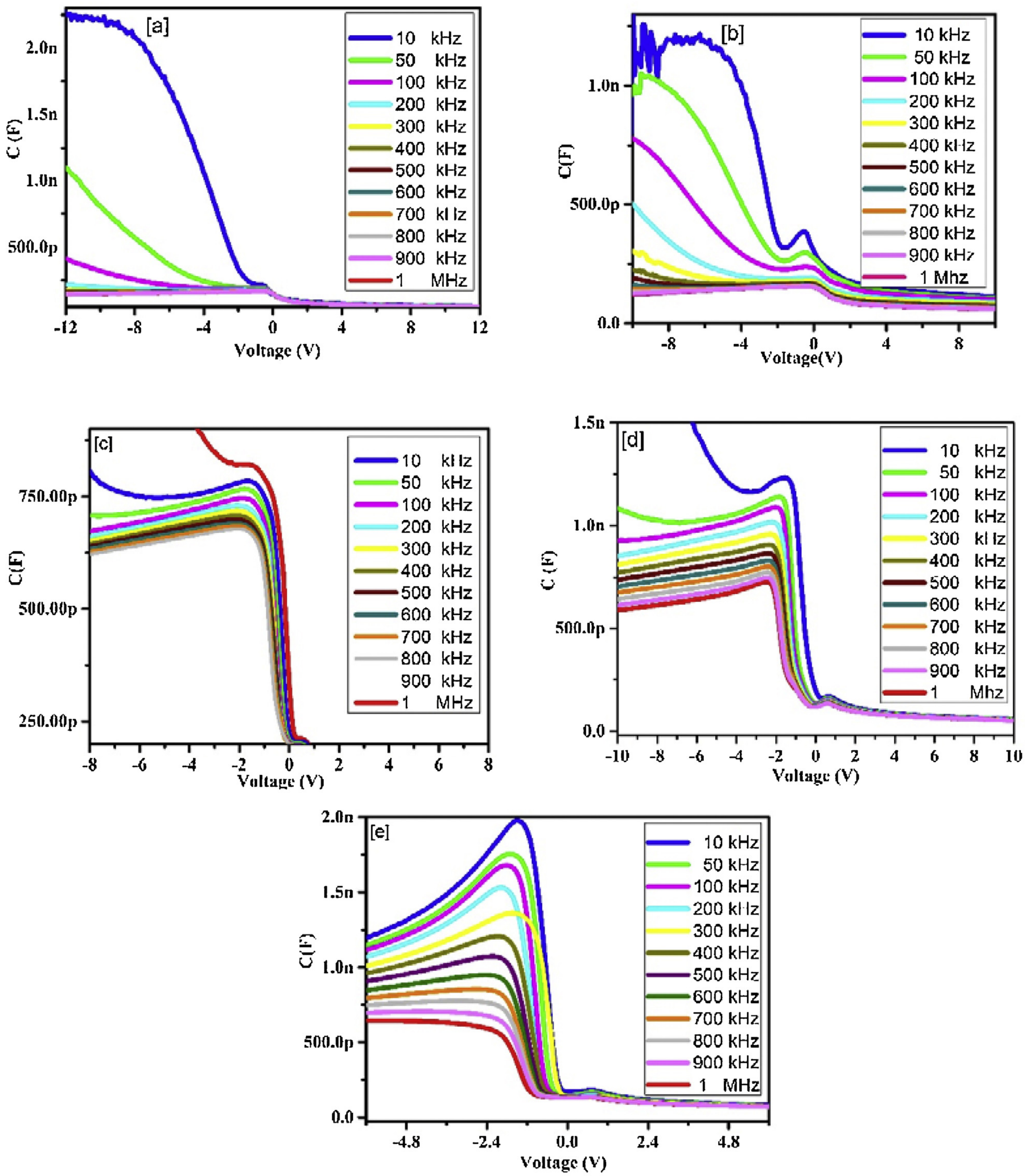

Fig. 8. *C–V* characteristics of the fabricated diodes (a) 0.005 (b) 0.01 (c) 0.03 (d) 0.05 (e) 0.1 GO:MB ratio.

composites were investigated using atomic force microscopy (AFM). The current–voltage (*I–V*) characteristics of the diodes were performed using a KEITHLEY 4200 semiconductor characterization system (SCS). Photo response measurements were performed using a solar simulator and KEITHLEY 4200 SCS. The intensity of the illumination was measured using a solar power meter (TM-206). The schematic diagram of the fabricated diode is shown in Fig. 1.

3. Results and discussion

AFM images of the GO:MB films are shown in Fig. 2. As seen in AFM images of the composites, the GO/MB composites shows nano-sized particles evenly distributed on the surface of the samples. *I–V* characteristics of the Al/p-Si/GO doped MB/Au photodiodes were measured under dark and various illumination intensities. Fig. 3(a–e) shows the plots of the Al/p-Si/GO doped MB/

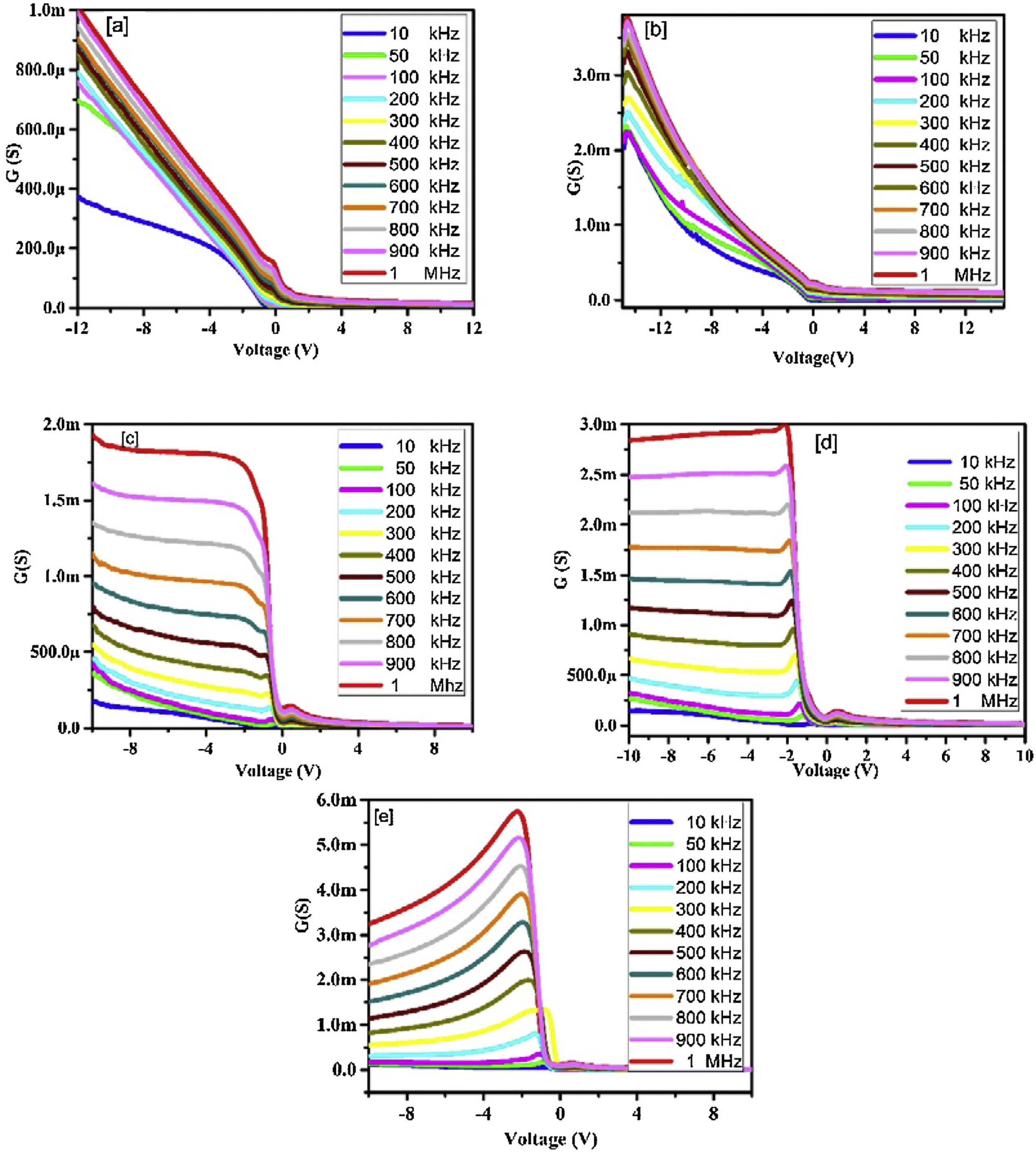

Fig. 9. *G–V* characterization of the fabricated diodes (a) 0.005 (b) 0.01 (c) 0.03 (d) 0.05 (e) 0.1 GO:MB ratio.

Au diodes, to analyze the charge transport and photo-conducting mechanisms. As seen in the figure, for all doping (x = GO: MB; x = 0.005, 0.01, 0.03, 0.05 and 0.10) in the reverse region, the current increases with increasing solar illumination intensity, while in the forward region, the current does not change with illumination. This behavior indicates that the diodes fabricated works in reverse bias region and the separation of electron-hole pairs in reverse bias region is larger than that of forward region [23–25]. Clearly, the rectifying properties of the diodes are dependent on the dopant and they exhibit conventional photo-conducting behavior [26].

The *I–V* characteristics of such a device can be expressed as [27];

$$I = I_0 \exp\left(\frac{q(V - IR_s)}{nkT}\right) \quad (1)$$

where n is the ideality factor, q is the electronic charge, k is the Boltzmann constant, T is the temperature, V is the applied voltage, R_s is the series resistance and I_0 is the reverse saturation current given by [27,28];

$$I_0 = AA^{*}T^2 \exp\left(\frac{-q\phi_b}{kT}\right) \quad (2)$$

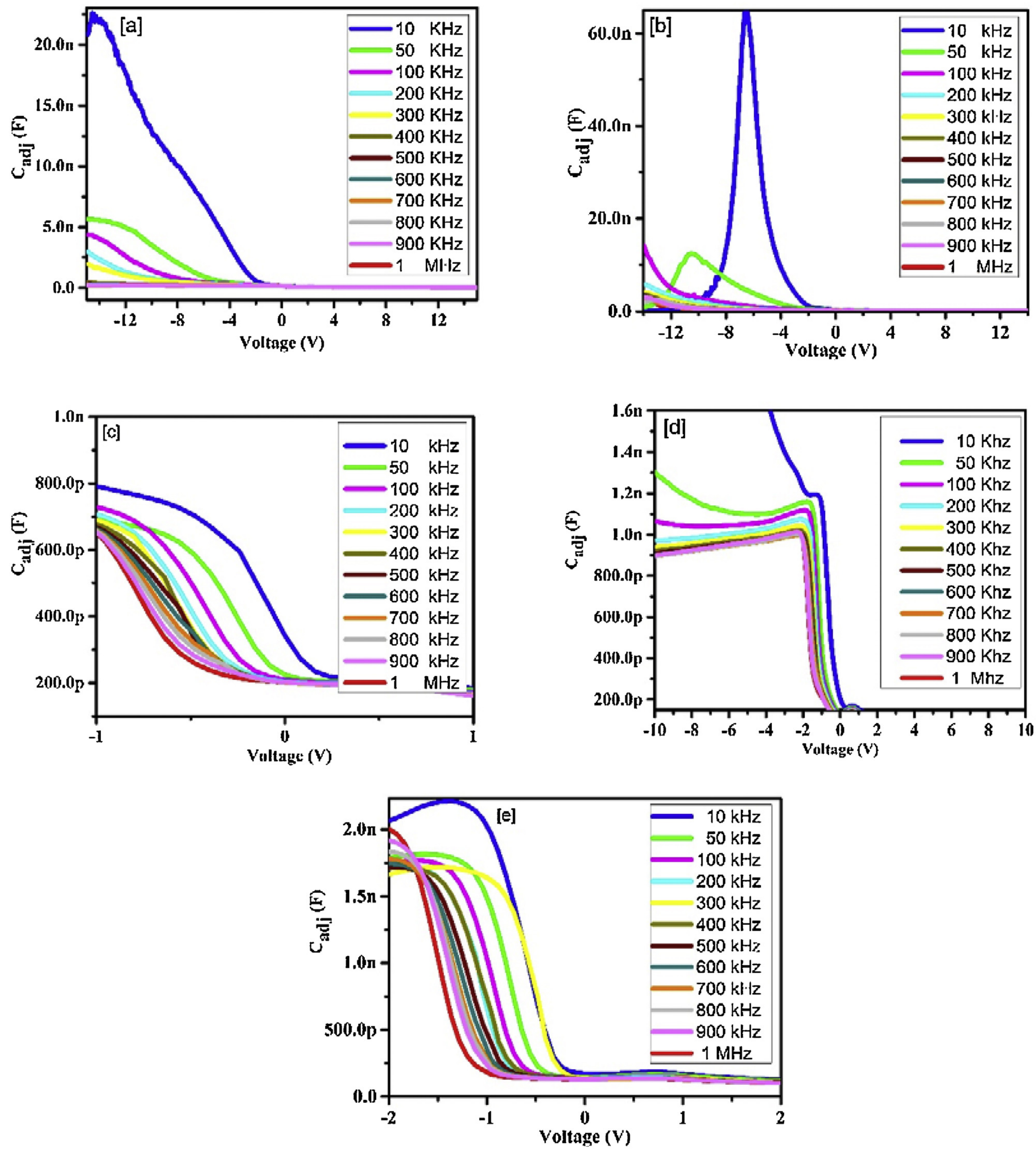

Fig. 10. C_{ADJ}–V characterization of the fabricated diodes (a) 0.005 (b) 0.01 (c) 0.03 (d) 0.05 (e) 0.1 GO: MB ratio.

where A is the active device area, A^* is the Richardson constant (32 A/cm^{2}K^2 for p-Si) and $\phi_b$the barrier height [29]. The experimental values of barrier height (ϕ_b) and ideality factor (n) were determined from the intercepts and slopes of the forward bias, as described by Phan et al. [30].

Obtained results presented in Fig. 4, shows the ideality factor of the diodes ranging from 3.97 to 9.52. It was found that the diode with GO: MB ratio of 0.03 had the highest ideality factor. Evidently, the ideality factor of the fabricated diodes is much larger than that of an ideal diode. Such a behavior suggests that the transport mechanism consists of defect-assisted tunneling with conventional electron–hole recombination [31]. This can also be explained using the interface states, inhomogenities of the barrier height and series resistance [32–34]. Clearly, the ideality factor and barrier height of the diodes changes with MB doping. Also the obtained trends for both ideality factor and barrier height are in agreement, suggesting that they are both affected by GO doping. Hendi [35] has prepared GO doped ZnO based diodes such as ZnO-GO/p-Si and ZnO-GO/n-Si, for various GO doping and concluded that the diode having 0.03 M ratio of GO: ZnO exhibited the highest photo-responsivity with 0.5 A/W under 100 mW/cm^2. Other published work by Fan et al., [36] and Li et al. [14] showed an

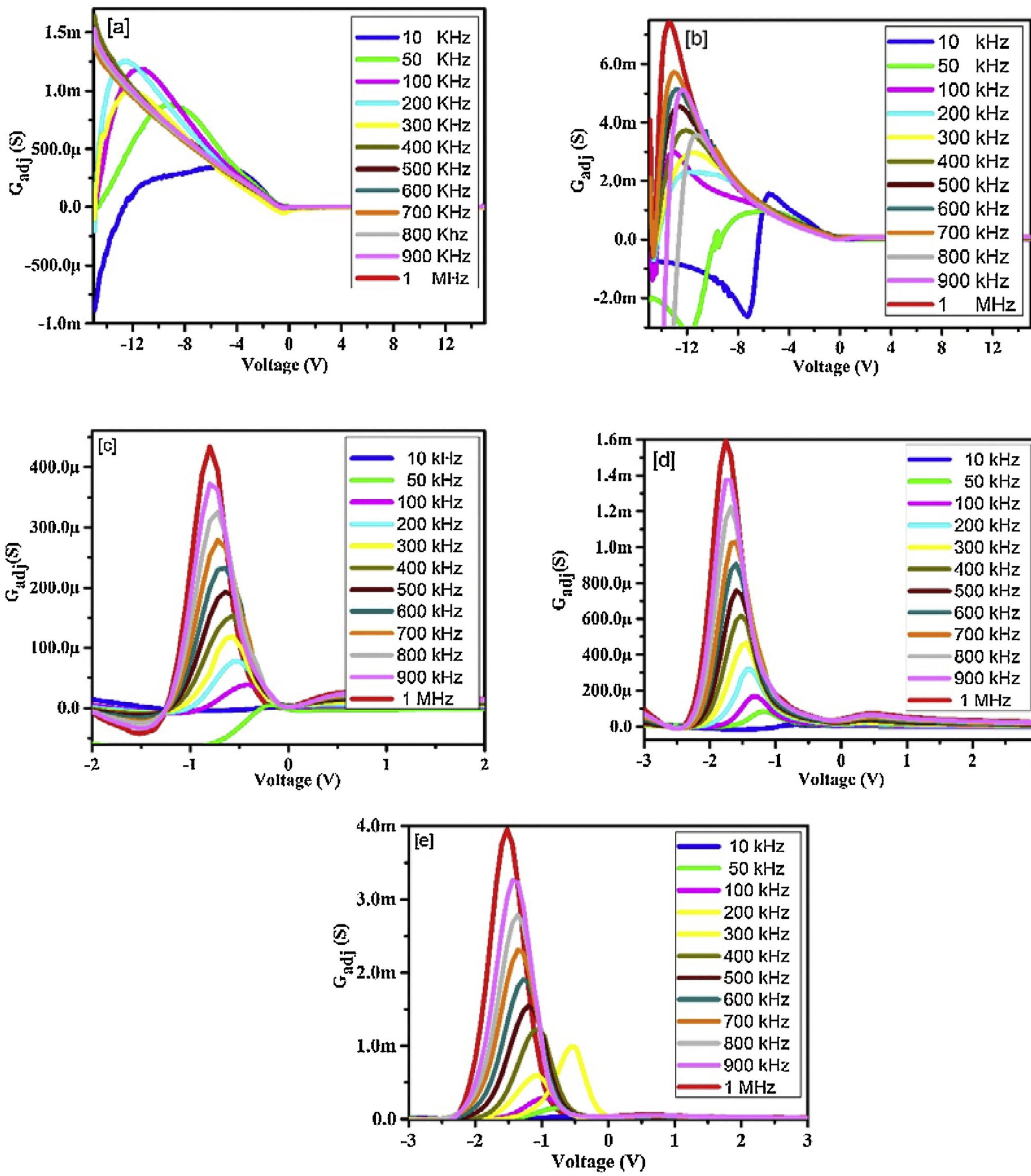

Fig. 11. G_{ADJ}–V characterization of the fabricated diodes (a) 0.005 (b) 0.01 (c) 0.03 (d) 0.05 (e) 0.1 GO: MB ratio.

ideality factor between 2 and 5.5 for the graphene–silicon based Schottky junction diodes and barrier height of about 0.78 eV for Schottky barrier based on graphene sheet and n-silicon for solar cells, respectively.

The open circuit voltage (V_{oc}) and short circuit current (I_{sc}) of the diode under 100 mW/cm^2 illumination is summarized in Table 1. Similar value has been reported by Itoh et al. [37]. The photosensitivity for the diodes is defined as the ratio of the photocurrent to the dark current, I_{photo}/I_{dark} at -10 V. The calculated photosensitivity for the fabricated are shown in Table 1. The highest photosensitivity was observed for the diode having 0.03 GO: MB ratio with I_{photo}/I_{dark} ratio of 8.67×10^3 at 100 mW/cm^2 under -10 V. The rectification ratio (*RR*) is determined as the ratio of the forward current (I_f) to the reverse current (I_r) at ±10 V applied voltage [38]. The observed values are shown in Table 1, it can be seen that the fabricated diodes exhibit rectification ratio ratios of the order of 10^4, such high values have been reported by others also [39,40].

To further assess the photosensitivity behavior of the diode, the variation of photocurrent with illumination intensity was investigated for the fabricated photodiodes. As a representative plot, photoconduction mechanism of the diode having 0.03 GO:MB ratio

Please cite this article in press as: A. Mekki, et al., Graphene controlled organic photodetectors, Synthetic Met. (2016), http://dx.doi.org/10.1016/j.synthmet.2016.03.015

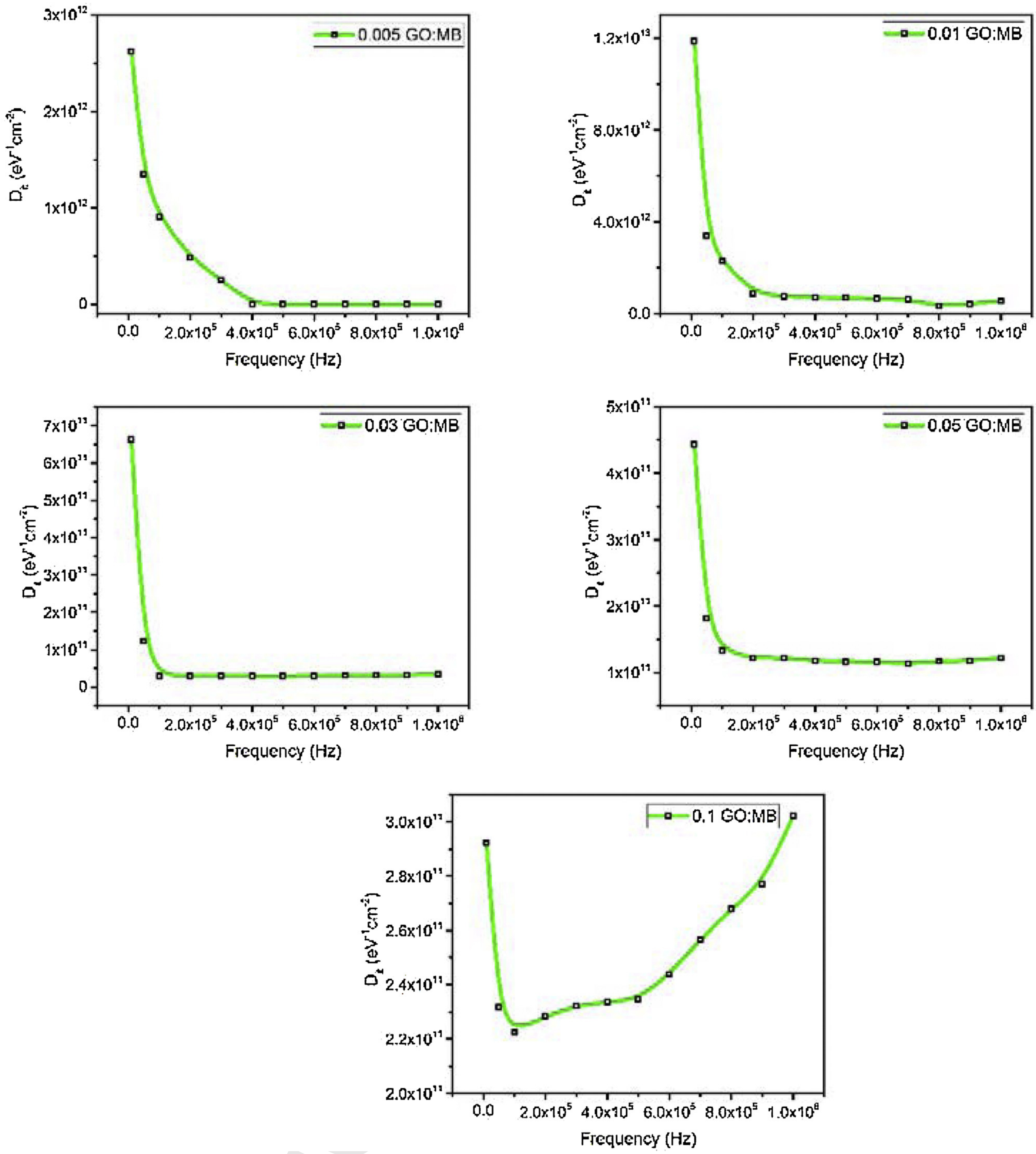

Fig. 12. Plot of *Dit* vs. frequency for the fabricated diodes (a) 0.005 (b) 0.01 (c) 0.03 (d) 0.05 (e) 0.1 GO: MB ratio.

is depicted in Fig. 5. The photoconducting mechanism of the diodes can be analyzed by the following relation [41]:

$$I_{PH} = KP^{m} \quad (3)$$

where, I_{PH} is the photocurrent, K is a constant, m is an exponent and P is the illumination intensity.

The value of m was determined from the slope of $\log(I_{PH})$ vs. $\log(P)$ plot. The obtained m (1.6) value indicates that the photocurrent exhibited a super linear behavior. This behavior supports views of other publications, which suggests that the photoconduction mechanism of the fabricated diode has a super linear correlation to the photoconductivity on intensity [42–44]. The super linear behavior is due to the recombination mechanism of state which have more cross section for holes than electrons [44].

To further investigate the photoconduction mechanism of the diodes, the widely used transient photocurrent technique was employed. The transient photocurrent characteristics of the photodiodes to pulsed light irradiation were performed under illumination of various light intensities (10, 30, 60, 80 and 100 mW/cm^2), and is shown in Fig. 6. As evident from Fig. 6(a-e), the fabricated photodiodes show reversible switching between high and low conductance, when light illumination was turned on and

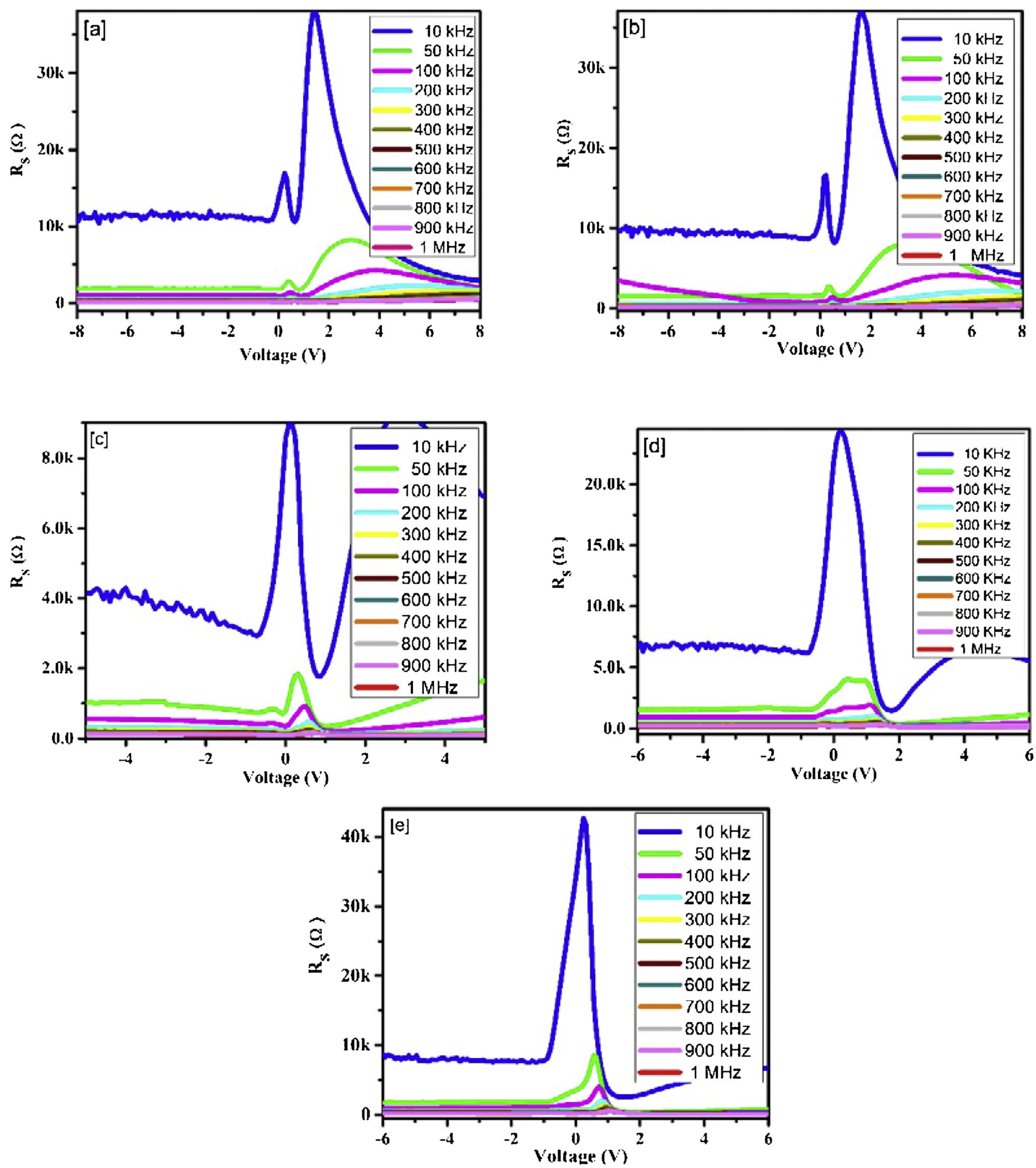

Fig. 13. R_s–V characterization of the fabricated diodes (a) 0.005 (b) 0.01 (c) 0.03 (d) 0.05 (e) 0.1 GO: MB ratio.

off. This phenomenon can be explained on the basis of charge carriers. The "on state" increases the number of free charge carriers, causing the photocurrent electron to increase, while the "off state" causes the decay of the photocurrent which is due to trapping of the charge carriers in the deep levels [45–47]. This behavior confirms the photodiode behavior.

Fig. 7 shows the transient capacitance (C-t) plots of the fabricated diodes. This is used to study the photocapacitance properties of the diode. As seen in Fig. 7(a-e), for all fabricated diodes, the capacitance increases at "on state" and decreases to its original state at "off state". The highest photocapacitance was observed for the diode having 0.1 GO:MB ratio at 10 kHz and illumination of 100 mW/cm^2. The photocapacitance gain was found to be about 3 for the diode having 0.1 GO:MB ratio. This behavior can be explained on the basis of interface charge carriers, which follows the frequency of the applied field at lower frequencies. The observed increase and decrease of the photocapacitance at low frequencies suggests that the fabricated diodes can be used in low frequency application. The effect of voltage and frequency on the capacitance (C–V–f) of the diodes were studied to further characterize the junction properties. As seen in Fig. 8(a-e), the capacitance of the photodiode for all the fabricated devices

Please cite this article in press as: A. Mekki, et al., Graphene controlled organic photodetectors, Synthetic Met. (2016), http://dx.doi.org/10.1016/j.synthmet.2016.03.015

does not change with frequency at the positive voltage. However, the capacitance changes with applied voltage and frequency at the negative voltage, decreasing with increasing frequency. On the other hand, the conductance of the diodes increases with increasing frequency, (G–V–f), Fig. 9(a-e). The observed peaks in Fig. 8 decreases in magnitude with increasing frequency, this behavior is attributed to the existence of interface states [48]. Clearly, the interface charges have minimal effects on the capacitance of the fabricated diodes at higher frequencies.

In order to analyze the interface states of the fabricated diodes, the C-V-f and G-V-f characteristics of the photo diodes were corrected with the series resistance by the following relation [49–51]:

$$C_{adj} = \frac{\left[G_m^2 + (\omega C_m)^2\right] C_m}{a^2 + (\omega C_m)^2} \tag{4}$$

$$G_{adj} = \frac{\left[G_m^2 + (\omega C_m)^2\right] a}{a^2 + (\omega C_m)^2} \tag{5}$$

And

$$a = G_m - \left[G_m^2 + (\omega Cm)^2\right] R_s \tag{6}$$

where C_{ADJ}–V and G_{ADJ}–V are series resistance compensated capacitance and conductance respectively. The effects of frequency on the C_{ADJ} –V and G_{ADJ}–V plots are shown in Figs. 10 and 11 respectively. From Fig. 11, it is observed that the G_{ADJ} peak intensity decreases with increasing frequency, while the peak also shifts towards higher negative voltage. It is further noted that the C_{ADJ}–V plots (Fig. 10) exhibited similar behavior, confirming the presence of interface states. The density of interface states (D_{it}) can be estimated using the Hill-Coleman method, given by [49,51,52]:

$$D_{it} = \left(\frac{2}{qA}\right)\left[\frac{(G_{\max}/\omega)}{\left[(G_{\max}/\omega C_{ox})^2 + (1 - C_m/C_{ox})^2\right]}\right] \tag{7}$$

where C_m is the measured capacitance, $(G_m/\omega)_{\max}$ is the measured conductance, C_{ox} is the capacitance of the insulator layer, A is the area of the diode and ω is the angular frequency. The D_{it} values for fabricated diodes were calculated and shown in Fig. 12. It can be inferred from Fig. 12 that the D_{it} value decreases with increasing frequency for all fabricated diodes, except for the 0.1 GO: MB. High D_{it} values is responsible for the non-ideal behavior of the I–V and C–V characteristics of the diodes and at low frequencies the interface states densities strongly depend on frequency.

Fig. 13 shows the plot of R_s–V of the fabricated photo diodes. The R_s values are calculated from the capacitance and conductance values in the accumulation region [53]. The observed peak intensity decreases and shifts with increasing frequency, which is due to the interface charges following the frequency of the applied voltage.

4. Conclusions

Al/p-Si/GO doped MB/Au photodiodes exhibited both the photoconductivity and photocapacitance behavior. The device parameters were determined using direct current and impedance measurements. The transient photocurrent of the device was shown to depend on light intensity, increasing with increasing light intensities. The photoresponse of the fabricated diodes changes with changing GO doping, and the sample with 0.03 GO: MB ratio exhibited the highest photoresponse. C–V–f and G–V–f measurements were explained on the basis of interface states, confirming that capacitance and conductance vary with applied voltage and frequency. It is evaluated that Al/p-Si/GO doped MB/Au devices can be used as a photosensor for solar tracking applications.

Acknowledgments

Three of the authors (AM, KH & FY) would like to thank The Deanship of Scientific Research at KFUPM for supporting this work under project #IN141009.

References

[1] D. Chen, H. Feng, J. Li, Graphene oxide preparation, functionalization, and electrochemical applications, Chem. Rev. 112 (2012) 6027–6053.
[2] A.K. Geim, K.S. Novoselov, The rise of graphene, Nat. Mater. 6 (2007) 183–191.
[3] P. Avouris, Z. Chen, V. Perebeinos, Carbon-based electronics, Nat. Nanotechnol. 2 (2007) 605–615.
[4] Chuang, S., (Nature Publishing Group, 1995).
[5] K.S. Novoselov, et al., Electric field effect in atomically thin carbon films, Science 306 (2004) 666–669.
[6] P. Blake, et al., Making graphene visible, Appl. Phys. Lett. 91 (063124) (2007).
[7] A.H. Castro Neto, F. Guinea, N.M.R. Peres, K.S. Novoselov, A.K. Geim, The electronic properties of graphene, Rev. Mod. Phys. 81 (2009) 109–162.
[8] A.K. Geim, Graphene status and prospects, Science 324 (2009) 1530–1534.
[9] S. Dusari, N. Goyal, M. Debiasio, A. Kenda, Raman spectroscopy of graphene on AlGaN/GaN heterostructures, Thin Solid Films 597 (2015) 140–143.
[10] F. Xia, T. Mueller, Y.-m. Lin, A. Valdes-Garcia, P. Avouris, Ultrafast graphene photodetector, Nat. Nano 4 (2009) 839–843.
[11] J. Guo, Y. Yoon, Y. Ouyang, Gate electrostatics and quantum capacitance of graphene nanoribbons, Nano Lett. 7 (2007) 1935–1940.
[12] E.J.H. Lee, K. Balasubramanian, R.T. Weitz, M. Burghard, K. Kern, Contact and edge effects in graphene devices, Nat. Nanotechnol. 3 (2008) 486–490.
[13] Y.M. Lin, Operation of graphene transistors at gigahertz frequencies, Nano Lett. 9 (2009) 422–426.
[14] X. Li, et al., Graphene-on-silicon Schottky junction solar cells, Adv. Mater. 22 (2010) 2743–2748.
[15] K. Ihm, et al., Number of graphene layers as a modulator of the open-circuit voltage of graphene-based solar cell, Appl. Phys. Lett. 97 (032113) (2010).
[16] X. Lv, et al., Photoconductivity of bulk-Film-Based graphene sheets, Small 5 (2009) 1682–1687.
[17] J.I. Paredes, S. Villar-Rodil, A. Martínez-Alonso, J.M.D. Tascón, Graphene oxide dispersions in organic solvents, Langmuir 24 (2008) 10560–10564.
[18] D.R. Dreyer, S. Park, C.W. Bielawski, R.S. Ruoff, The chemistry of graphene oxide, Chem. Soc. Rev. 39 (2010) 228–240.
[19] O.A. Al-Hartomy, R.K. Gupta, A.A. Al-Ghamdi, F. Yakuphanoglu, High performance organic-on-inorganic hybrid photodiodes based on organic semiconductor-graphene oxide blends, Synth. Met. 195 (2014) 217–221.
[20] M.A. Zanjanchi, S. Sohrabnezhad, Evaluation of methylene blue incorporated in zeolite for construction of an optical humidity sensor, Sens. Actuators B 150 (2005) 502–507.
[21] W.S. Hummers, R.E. Offeman, Preparation of graphitic oxide, J. Am. Chem. Soc. 80 (1958) 1339–1339.
[22] H.A. Becerril, et al., Evaluation of solution-processed reduced graphene oxide films as transparent conductors, ACS Nano 2 (2008) 463–470.
[23] M.A. Mentzer, Applied Optics Fundamentals and Device Applications: Nano, MOEMS, and Biotechnology, CRC Press, 2011.
[24] E.H. Nicollian, J.R. Brews, MOS (Metal Oxide Semiconductor) Physics and Technology, Wiley, 1982.
[25] M. Fukuda, Optical Semiconductor Devices, Wiley, 1999.
[26] H. Aydin, et al., A novel type heterojunction photodiodes formed junctions of Au/LiZnSnO and LiZnSnO/p-Si in series, J. Alloys Compd. 625 (2015) 18–25.
[27] S.M. Sze, K.K. Ng, Physics of Semiconductor Devices, Wiley, 2006.
[28] M. Ilhan, Electrical characterization of Al/fluorescein sodium salt organic semiconductor/Au diode by current-voltage and capacitance-voltage methods, J. Mater. Electron. Devices 1 (2015) 15–20.
[29] S. Altındal, On the origin of increase in the barrier height and decrease in ideality Si (MIS) Schottky −/p2factor with increase temperature in Ag/SiO_2 barrier diodes (SBDs), J. Mater. Electron. Devices 1 (2015) 42–47.
[30] D.T. Phan, et al., Photodiodes based on graphene oxide–silicon junctions, Sol. Energy 86 (2012) 2961–2966.
[31] K. Mohanta, S.K. Batabyal, A.J. Pal, Organization of organic molecules with inorganic nanoparticles: hybrid nanodiodes, Adv. Funct. Mater. 18 (2008) 687–693.
[32] I.S. Yahia, F. Yakuphanoglu, S. Chusnutdinow, T. Wojtowicz, G. Karczewski, Photovoltaic characterization of n-CdTe/p-CdMnTe/GaAs diluted magnetic diode, Curr. Appl. Phys. 13 (2013) 537–543.
[33] T. Adem, Comparative study of the electrical properties of Au/n-Si (MS) and Au/Si 3 N 4/n-Si (MIS) Schottky diodes, Chin. Phys. B 22 (068402) (2013).
[34] H. Özerli, İ. Karteri, Ş. Karataş, Ş. Altindal, The current–voltage and capacitance–voltage characteristics at high temperatures of Au Schottky contact to n-type GaAs, Mater. Res. Bull. 53 (2014) 211–217.

[35] A.A. Hendi, Electrical and photoresponse properties of graphene oxide:ZnO/Si photodiodes, J. Alloys Compd. 647 (2015) 259–264.
[36] G. Fan, et al., Graphene/Silicon nanowire schottky junction for enhanced light harvesting, ACS Appl. Mater. Interfaces 3 (2011) 721–725.
[37] E. Itoh, H. Nakamichi, K. Miyairi, Surface potential measurement of organic photo-diode consisting of fullerene/copper phthalocyanine double layered device, Thin Solid Films 516 (2008) 2562–2567.
[38] X. Ho, et al., Theoretical and experimental studies of Schottky diodes that use aligned arrays of single-walled carbon nanotubes, Nano Res. 3 (2010) 444–451.
[39] J.D. Hwang, K.S. Lee, A high rectification ratio nanocrystalline p–n junction diode prepared by metal-Induced lateral crystallization for solar cell applications, J. Electrochem. Soc. 155 (2008) H259–H262.
[40] A.K. Mahapatro, S. Ghosh, Schottky energy barrier and charge injection in metal/copper–phthalocyanine/metal structures, Appl. Phys. Lett. 80 (4840) (2002).
[41] M. El-Kemary, M. Gaber, Y.S. El-Sayed, Y. Gheat, Photoinduced interaction of CdSe quantum dot with coumarins, J. Lumin. 159 (2015) 26–31.
[42] R.W. Smith, A. Rose, Space-charge-limited currents in single crystals of cadmium sulfide, Phys. Rev. 97 (1955) 1531–1537.
[43] S.K. Mishra, R.K. Srivastava, S.G. Prakash, R.S. Yadav, A.C. Panday, Photoluminescence and photoconductive characteristics of hydrothermally synthesized ZnO nanoparticles, Opto-Electron. Rev. 18 (4) (2016) 467–473.
[44] R. Revi, P. Purkayastha, P.K. Kalita, R. Sarma, H.J. Das, B.K. Sarma, Photoelectric properties of CdS thin Film prepared by chemical bath deposition, Indian J. Pure Appl. Phys. 45 (2007) 624–627.
[45] F. Yakuphanoglu, et al., Ferroelectric $Bi_{3.25}La_{0.75}Ti_3O_{12}$ photodiode for solar cell applications, Sol. Energy Mater. Sol. Cells 133 (2015) 69–75.
[46] R.H. Al Orainy, A.A. Hendi, Fabrication and electrical characterization of CdO/p-Si photosensors, Microelectron. Eng. 127 (2014) 14–20.
[47] B. Varghese, et al., Electrical and photoresponse properties of Co_3O_4 nanowires, J. Appl. Phys. 111 (104306) (2012).
[48] M. Çakar, Y. Onganer, A. Türüt, The nonpolymeric organic compound (pyronine-B)/p-type silicon/Sn contact barrier devices, Synth. Met. 126 (2002) 213–218.
[49] Ahmed A. Al-Ghamdi, R.K. Gupta, Yusuf Al-Turki, F. El-Tantawy, F. Yakuphanoglu, Efficiency enhancement and transient photocapacitance characteristics of the silicon solar cell by graphene oxide, J. Mater. Electron. Devices 1 (2015) 11–14.
[50] E.H. Nicollian, A. Goetzberger, A.D. Lopez, Expedient method of obtaining interface state properties from MIS conductance measurements, Solid-State Electron. 12 (1969) 937–944.
[51] İ. Dökme, Ş. Altındal, T. Tunç, İ. Uslu, Temperature dependent electrical and dielectric properties of Au/polyvinyl alcohol (Ni, Zn-doped)/n-Si Schottky diodes, Microelectron. Reliab. 50 (2010) 39–44.
[52] W.A. Hill, C.C. Coleman, A single-frequency approximation for interface-state density determination, Solid-State Electron. 23 (1980) 987–993.
[53] F. Yakuphanoglu, Electrical characterization and device characterization of ZnO microring shaped films by sol–gel method, J. Alloys Compd. 507 (2010) 184–189.